Contribution of the electron redistribution effect to the piezoelectric constant due to the bond bending in tetrahedral crystals

Takehiko Hidaka
Electrotechnical Laboratory, 5-4-1, Mukodai, Tanashi-shi, Tokyo, Japan
(Received 19 September 1977)

The electron-cloud distortion of GaAs and ZnSe under uniaxial stress is discussed using the Chadi-Cohen empirical linear-combination-of-atomic-orbitals band theory. The electron localizability $\lambda = (a^2 - b^2)/(a^2 + b^2)$, where a is the weight of the anion atomic wave function and b is that of the cation atomic wave function in the valence-state wave function $\psi_v = a\psi^\alpha + b\psi^\beta$, changes with the bond bending of the tetrahedral structure induced by [111]-directional external stress. This electron redistribution effect gives a large contribution to the piezoelectric constant. e_b^*/e_0 is 0.32 for GaAs and 0.27 for ZnSe, e_b^* being the effective charge due to the bond-bending effect.

I. INTRODUCTION

The piezoelectric constant is one of the most important parameters of lattice dynamics. The most striking aspect of the piezoelectric constant of zinc-blende-type crystals is that its sign reverses on going from III-V compounds to II-VI compounds.

Martin[1] gave the theory of the piezoelectric effective charge e_{14}^*; it is the sum of e_T^* and Q, where e_T^* is transverse optical charge and Q is the quadrupole moment of the unit cell under stress. For the definition of e_{14}^* and Q, refer to Martin's paper. Several authors[2-4] asserted that the ionicity change, or the electron redistribution effect, due to the external strain, contributes to the piezoelectric constant. The idea of an electron redistribution effect seems to be consistent with Martin's theory, as discussed below. Bennett and Maradudin,[5] and Lennoo and Decarpigny[6] calculated the e_T^* values for tetrahedral crystals. The electron-cloud distortion due to the lattice vibration is given from

$$|\psi_v\rangle = |\psi_v^0\rangle + [|\psi_e^0\rangle\langle\psi_e^0| V|\psi_v^0\rangle/(E_e - E_v)], \tag{1}$$

where $|\psi_v^0\rangle$ and $|\psi_e^0\rangle$ are the wave functions of the valence and excited states, respectively. E_e and E_v are their energy levels, V is the interaction operator between the lattice vibration and the electron (deformation potential). The superscript 0 shows nonperturbed states. We assume that

$$\psi_v^0 = a\psi^\alpha + b\psi^\beta, \quad \psi_e^0 = b\psi^\alpha - a\psi^\beta, \tag{2}$$

where ψ^α and ψ^β are the atomic wave functions of the anion and cation in tetrahedral compounds, respectively, and a and b are the weights of them. Then, the electron localizability λ is defined naturally as

$$\lambda = (a^2 - b^2)/(a^2 + b^2). \tag{3}$$

λ changes with the lattice vibration as

$$\Delta\lambda = \lambda - \lambda_0 = 2J/(1 + b^2/a^2), \tag{3'}$$

using Eqs. (1) and (2), where λ_0 is the electron localizability of the unperturbed state and $J = \langle\psi_e^0| V|\psi_v^0\rangle/(E_e - E_v)$. The electron-cloud distortion in e_T^* is described by the change in λ. The change of λ contributes to the piezoelectric constant through e_T^*. Moreover, it is expected that the quadrupole moment Q of Martin includes the effect of the electron-cloud distortion due to the lattice distortion.

Harrison[4] discussed the effect of the change in electron polarity due to the external stress on the piezoelectric constant. He assumed that the electron-cloud-distortion effect is due *only* to the change in bond length. In general, the distortion $\Delta\rho$ of the electron distribution ρ induced by the external strain δ given in Fig. 1 is

$$\Delta\rho = \left(\frac{\partial\rho}{\partial d_0}\frac{\partial d_0}{\partial\delta} + \frac{\partial\rho}{\partial\theta_b}\frac{\partial\theta_b}{\partial\delta}\right)\delta, \tag{4}$$

where d_0 is the bond length and θ_b is the bond angle defined in Fig. 1(a). The first term of Eq. (4) represents the bond-stretching effect, and the second term the bond-bending effect. Harrison treated only the first term. No clear reasons exist that allow us to ignore the second term of Eq. (4). The bond-bending effect may correspond to the quadrupole moment Q because the cations (indicated by β in Fig. 1) move along with the plane perpendicular to the direction of the external stress.

In this paper, we discuss the effect of the change in the electron localizability λ due to bond-bending, using the empirical linear-combination-of-atomic-orbitals (ELCAO) band theory developed by Chadi and Cohen.[7]

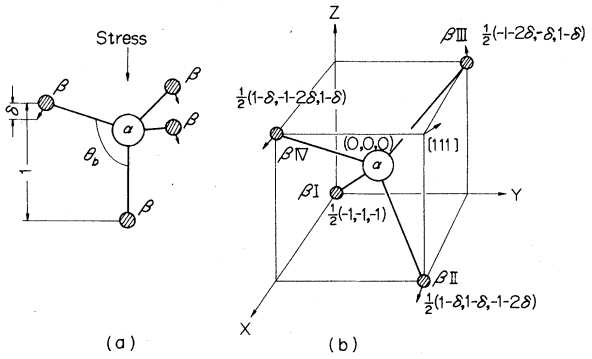

FIG. 1. (a) Unit tetrahedron and the strain δ induced by [111] directional uniaxial stress. α stands for anion and β for cation. θ_b is the bond angle. (b) Positions of respective atoms in the unit cell of zinc-blende structure under strain.

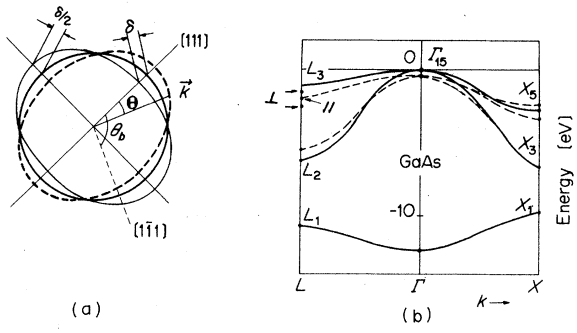

FIG. 2. (a) Simplified Brillouin zone of zinc-blende-type crystals under [111]-directional strain δ. The Brillouin zone expands by $1+\delta$ in the [111] direction, and it contracts by $1-\frac{1}{2}\delta$ along the axis perpendicular to the [111] axis. Θ is the direction of the $\vec{k}$ vector. θ_b is the bond angle. (b) Valence-band structure of GaAs. The dashed lines show the change under the strain δ. The X_5 state is split into two levels. The L_3 state is also split at the $L^{\perp}$ point (see text). Γ_{15} is slightly leveled down. L_2 is slightly leveled up. The s-like deep band (L_1-Γ_1-X_1) scarcely changes.

II. ELCAO BAND THEORY AND THE ELECTRON LOCALIZABILITY UNDER STRESS

In this section, we calculate λ under stress using the ELCAO band method. The definition of λ is similar to that of Harrison's α_p.[4] However, the calculation method is different from his; we use λ independently. The reason we use the linear-combination-of-atomic-orbitals (LCAO) method is that the value of λ and its change with stress are deduced directly rather than through another band-calculation method such as the pseudopotential band theory. In the simplest LCAO method, we use eight atomic wave functions s^{α}, p_x^{α}, p_y^{α}, p_z^{α}, s^{β}, p_x^{β}, p_y^{β}, and p_z^{β} as basis functions. α stands for anion and β for cation. Also, we consider only the nearest-neighbor atoms interactions in the eight-by-eight eigenvalue problem.[7] For details refer to Ref. 7.

The stress is applied along the [111] axis, as in Fig. 1. The strain δ is defined as in Fig. 1(a). We assume that the bond lengths do not change under stress; only the bond angle θ_b is assumed to change. Kleinman's ζ is assumed to be unity for the value of the second term in Eq. (4). Fig. 1(b) shows the atomic positions with strain δ along the [111] direction. These atomic positions are deduced easily by a simple geometrical consideration, the details of which are omitted for simplicity. The off-diagonal elements in the eigenvalue problem, under stress, are given as follows. For example, $\langle s^{\alpha}|h|p_x^{\beta\mathrm{II}}\rangle$ between the anion and the βII cation in Fig. 2(b) is

$$\langle s^{\alpha}|h|p_x^{\beta\mathrm{II}}\rangle = sp\sigma[(1-\delta)/\sqrt{3}\,]e^{i/2} \times[(1-\delta)k_x+(1-\delta)k_y+(-1-2\delta)k_z]a_0\,, \tag{5}$$

where $sp\delta/\sqrt{3}$ is the energy parameter between s^{α} and $p_x^{\beta\mathrm{II}}$ in Fig. 1, without distortion. $sp\sigma$ represents the σ bonding of s- and p_x-type wave functions. The factor of $(1-\delta)$ in Eq. (5) arises from the change in the s^{α}-$p_x^{\beta\mathrm{II}}$ interaction under the distortion δ. The change in the matrix elements of the secular equation is assumed to be caused by the change in bond angle only. The details are given by Slater and Koster,[8] and we omit them.

The Brillouin zone of the crystal under stress is also distorted. A simplified picture of it is shown in Fig. 2(a). In the [111] direction, the Brillouin zone is expanded by $1/(1-\delta)\approx 1+\delta$ because the lattice constant in this direction is contracted to $1-\delta$. In the direction perpendicular to the [111] axis, the Brillouin zone is contracted to $1-\frac{1}{2}\delta$ because the lattice constant in this direction is expanded to $1+\frac{1}{2}\delta$. The Poisson's ratio is assumed to be 2.0, in agreement with the assumption $\zeta=1$. In an arbitrary direction indicated by Θ in Fig. 2(a), the Brillouin-zone boundary changes by

$$1+\delta\cos^2\Theta-\tfrac{1}{2}\delta\sin^2\Theta\,, \tag{6}$$

times the original boundary size.

Now we calculate the valence band λ of Eq. (3) using the Chadi-Cohen parameters.[7] The results for the band energy is shown in Fig. 2(b). Table I gives the weights of the respective atomic wave functions in the respective valence-band positions for GaAs. a_s, b_s, a_p, and b_p are, respectively, the factors of the anion s-type, cation s-type, anion p-type wave functions. a_p and b_p are calculated from $a_p^2=a_{px}^2+a_{py}^2+a_{pz}^2$ and $b_p^2=b_{px}^2+b_{py}^2+b_{pz}^2$ in the

TABLE I. Weights of the atomic wave functions at the respective points of the Brillouin zone of GaAs. The definition of a_s^2, etc. is given in Sec. II. $\bar{\lambda}_s$ and $\bar{\lambda}_p$ are the weighted averages of λ for s-type and p-type valence-state wave functions. $\delta = 0$.

Point	a_s^2	b_s^2	a_p^2	b_p^2
Γ_1	0.543	0.457	0	0
Γ_{15}	0	0	0.96	0.04
X_1	0.792	0.003	0	0.204
X_3	0.002	0.776	0.22	0.001
X_5	0	0	0.712	0.289
L_1	0.653	0.238	0	0.108
L_2	0.067	0.446	0.343	0.144
L_3	0	0	0.808	0.192
	$\bar{\lambda}_s = 0.028$		$\bar{\lambda}_p = 0.466$	

respective valence wave function

$$\psi_v = a_s s^\alpha + a_{px} p_x^\alpha + a_{py} p_y^\alpha + a_{pz} p_z^\alpha + b_s s^\beta + b_{px} p_x^\beta + b_{py} p_y^\beta + b_{pz} p_z^\beta . \quad (7)$$

The λ's of s-type and p-type wave functions at the respective Brillouin-zone points are defined as

$$\lambda_s = (a_s^2 - b_s^2)/(a_s^2 + b_s^2) , \quad \lambda_p = (a_p^2 - b_p^2)/(a_p^2 + b_p^2) . \quad (8)$$

These are given in Table I for nondistorted GaAs, independently of the respective Brillouin-zone points. We emphasize the fact that the respective valence states each have a different λ value. This had not been recognized yet. The averages $\overline{\lambda_s}$ and $\overline{\lambda_p}$ over the Brillouin zone are assumed to be the weighted averages over all Γ, X, and L points in a unit Brillouin zone. There are six X points and eight L points. However, the zone boundary of an unit Brillouin zone belongs commonly to the next-nearest-neighbor Brillouin zone. Hence the weights of X and L points are, respectively, three and four times larger than for the Γ point. Altogether, the electron localizabilities $\overline{\lambda_s}$ and $\overline{\lambda_p}$ are 0.028 and 0.466, respectively. We further emphasize that the localizability of the s-type wave function is different from that of the p-type wave function. Table II shows values for ZnSe without distortions. Tetrahedral crystals have sp^3 bonding wave functions along the respective bonds in Fig. 1. The bond-electron localizability λ_b is defined as $\frac{1}{4}\overline{\lambda_s} + \frac{3}{4}\overline{\lambda_p}$, which is 0.357 for GaAs and 0.644 for ZnSe, without distortion. The factors $\frac{1}{4}$ and $\frac{3}{4}$ are the weights of s-type and p-type wave functions in the sp^3 bonding wave functions.

For the distorted state, the electron localizabilities $\overline{\lambda_s}$ and $\overline{\lambda_p}$ are also calculated as in Tables III and IV. The lattice distortion δ is assumed 0.05 for sample computer calculations. The dashed

TABLE II. Weights of atomic wave functions of ZnSe, with $\delta = 0$.

Point	a_s^2	b_s^2	a_p^2	b_p^2
Γ_1	0.789	0.211	0	0
Γ_{15}	0	0	0.984	0.016
X_1	0.915	0	0	0.085
X_3	0	0.521	0.479	0
X_5	0	0	0.82	0.18
L_1	0.869	0.074	0	0.055
L_2	0.014	0.361	0.544	0.081
L_3	0	0	0.905	0.095
	$\bar{\lambda}_s = 0.345$		$\bar{\lambda}_p = 0.744$	

lines in Fig. 2(b) show the valence-band energy change with δ. The Γ_1^v energy scarcely changes. The Γ_{15}^v point is slightly leveled down with very small splitting. The changes in X_1^v and X_3^v are very small, and the X_5^v state is split into two levels under [111] strain. For the [100] direction, $\cos\Theta = 1/\sqrt{3}$ so that the Brillouin-zone boundary does not change from Eq. (6). Also, the axes X, Y, and Z are equivalent to each other for [111] directional stress; all six X points in the Brillouin zone are equivalent.

Among the L points of the Brillouin zone, the

TABLE III. Weights of atomic wave functions of GaAs under uniaxial stress in the [111] direction. The strain δ in the [111] direction is assumed to be 0.05. The X_5 and L_3 states are split into two levels, respectively. $\parallel$ indicates the L point on the [111] axis (parallel) and $\perp$ the L point on the [$\bar{1}\bar{1}\bar{1}$] axis, etc. (perpendicular).

Point	a_s^2	b_s^2	a_p^2	b_p^2
Γ_1	0.543	0.456	0	0
Γ_{15}	0.01	0.007	0.972	0.011
X_1	0.79	0.003	0.001	0.206
X_3	0.004	0.775	0.220	0.001
X_5	0	0	0.696	0.306
X_5	0	0	0.732	0.269
$L_1^{\parallel}$	0.650	0.258	0	0.092
$L_2^{\parallel}$	0.067	0.416	0.357	0.160
$L_3^{\parallel}$	0	0	0.792	0.208
$L_3^{\parallel}$	0	0	0.791	0.209
$L_1^{\perp}$	0.651	0.236	0	0.112
$L_2^{\perp}$	0.076	0.457	0.338	0.138
$L_3^{\perp}$	0	0	0.792	0.208
$L_3^{\perp}$	0	0	0.800	0.200
	$\bar{\lambda}_s = 0.027$		$\bar{\lambda}_p = 0.500$	

TABLE IV. Weights of atomic wave functions of ZnSe under uniaxial stress. The strain δ is 0.05.

Point	a_s^2	b_s^2	a_p^2	b_p^2
Γ_1	0.787	0.213	0	0
Γ_{15}	0.006	0.011	0.977	0.006
X_1	0.916	0	0	0.084
X_3	0	0.52	0.48	0
X_5	0	0	0.803	0.197
X_5	0	0	0.841	0.159
$L_1^{\parallel}$	0.876	0.076	0	0.049
$L_2^{\parallel}$	0.011	0.334	0.560	0.094
$L_3^{\parallel}$	0	0	0.892	0.103
$L_3^{\parallel}$	0	0	0.892	0.103
$L_1^{\perp}$	0.865	0.075	0	0.060
$L_2^{\perp}$	0.018	0.373	0.538	0.071
$L_3^{\perp}$	0	0	0.898	0.102
$L_3^{\perp}$	0	0	0.891	0.108
	$\overline{\lambda_s}=0.343$		$\overline{\lambda_p}=0.764$	

point 111 is not equal to $11\bar{1}$ (or 111 and $1\bar{1}1$). The Brillouin-zone boundary in the [111] direction is expanded $1+\delta$ times, and in the $[11\bar{1}]$ direction is reduced $(1-\frac{1}{3}\delta)$ times because $\cos\Theta=\frac{1}{3}$ for the $[11\bar{1}]$ direction. We should calculate the 111 point and others such as the $11\bar{1}$ point independently. The [111]-directional L point is named $L^{\parallel}$ (parallel) and the others $L^{\perp}$ (perpendicular). The changes of L-point valence bands under the strain δ are also shown in Fig. 2(b). The point L_1^v changes scarcely. The point L_2^v is slightly leveled up (equally for the parallel and perpendicular). $L_3^{\parallel}$ is leveled down (no splitting) and $L_3^{\perp}$ is split into two states. $L_3^{\parallel}$ and $L_3^{\perp}$ are independently calculated. $\overline{\lambda_s}$ and $\overline{\lambda_p}$ are the weighted averages over all Γ, X, and L points. Table III gives the results for GaAs and Table IV the results for ZnSe. $\overline{\lambda_s}$ is scarcely changed with δ, and $\overline{\lambda_p}$ is 7% larger than that of the undistorted state. The fact that the deep valence band is not perturbed by the stress seems very reasonable in terms of Eq. (1). No theories published already have explained this situation.

III. CONTRIBUTION OF LOCALIZABILITY CHANGE TO PIEZOELECTRIC CONSTANT

Now we discuss the effect due to the change in λ under external stress upon the piezoelectric constant. We only discuss the second term of Eq. (4) in Sec. I. $\zeta=1$ is assumed for this reason.

With the strain δ of Fig. 1, the X, Y, and Z directions are equivalent to each other. The a_{px}, a_{py}, and a_{pz} values in Eq. (7) are equal. Also b_{px}, b_{py}, and b_{pz} are equal. Thus, $\overline{\lambda_p}$ for the [111]-directional bond is equal to that for perpendicular bonds such as the $[11\bar{1}]$ bond.

For distorted crystals under [111]-directional stress, sp^3 hybridization is destroyed because the bond angle θ_b in Fig. 1(a) no longer has the ideal value 109.5°. This situation is shown in Fig. 3. Figure 3(b) shows the structure under extremely high pressure (sp^2 wave function). The s-p hybrid ratios of the respective bonds in the distorted crystal are no longer equal to that of the ideal structure. With the $\delta=0.05$ strain in Fig. 1, the respective bond localizabilities are given by

$$\lambda_b^{\parallel}=0.152\overline{\lambda_s}+0.848\overline{\lambda_p}\ ,$$
$$\lambda_b^{\perp}=0.283\overline{\lambda_s}+0.717\overline{\lambda_p}\ , \tag{9}$$

where $\lambda_b^{\parallel}$ is the bond localizability of the parallel ([111] directional) bond, and $\lambda_b^{\perp}$ is that of the perpendicular ($[11\bar{1}]$ directional) bond. The factors of 0.152, etc., in Eq. (9) are deduced in the Appendix; namely, the localizability of the respective bonds changes with the change in s-p hybrid ratio. For GaAs one obtains $\lambda_b^{\parallel}=0.428$ and $\lambda_b^{\perp}=0.366$ with $\delta=0.05$ strain. Also for ZnSe, $\lambda_b^{\parallel}=0.699$ and $\lambda_b^{\perp}=0.644$. We emphasize the fact that the bond-electron localizability is anisotropic under external stress even if we assume that the bond length d_0 does not change. The anisotropy in the bond localizability $\lambda_b^{\parallel}-\lambda_b^{\perp}$ is 0.062 for GaAs and 0.055 for ZnSe.

When $\lambda_b^{\parallel}$ and $\lambda_b^{\perp}$ change, there appears electronic polarization in the unit tetrahedron. Figure 4 shows the electron-cloud motion with change in λ_b. We first consider the [111] (parallel) bond. For the $\lambda_b^{\parallel}=0$ bond (perfectly covalent), the electron cloud stands midway of the anion to cation bond. When $\lambda_b^{\parallel}$ is increased, the electrons are localized at the anion site. Thus, for $\Delta\lambda_b^{\parallel}=1.0$ (strictly covalent to strictly ionic), the electron cloud moves from the bond center to the anion-

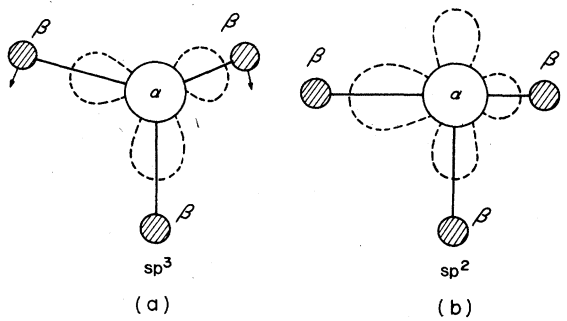

FIG. 3. (a) sp^3 wave function. (b) sp^2 wave function.

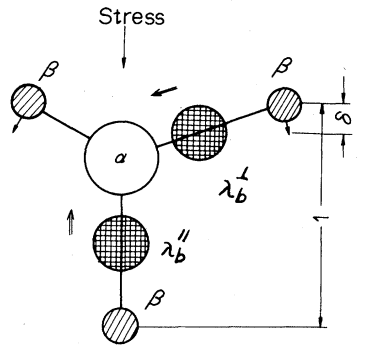

FIG. 4. Electron-cloud motion (⇒) with strain δ. The cross-hatched circles represent the valence-electron cloud. They are midway for $\lambda_b = 0$, and are localized at the anion site for $\lambda_b = 1.0$. $\parallel$ indicates the bond parallel to the [111]-directional stress, and $\perp$ indicates the bond perpendicular to it.

core position. $\Delta\lambda_b^{\parallel}$ shows the change of $\lambda_b^{\parallel}$ with the distortion. The electronic dipole moment generated together with $\Delta\lambda_b^{\parallel}$ is then

$$2(0.75/2)\Delta\lambda_b^{\parallel} = 0.75\Delta\lambda_b^{\parallel} , \tag{10}$$

where the first factor of 2 shows the electron number per one bond, the factor 0.75/2 means that the bond size is 0.75 (the unit cell is shown in Fig. 1) and the 2 in the denominator means that the electron-cloud moves a half of the bond length with $\Delta\lambda_b^{\parallel} = 1.0$. Moreover, for the perpendicular bond the generated dipole moment is

$$-2[3(0.25 - \delta/2)]\Delta\lambda_b^{\perp} , \tag{11}$$

where the minus sign means that the effect due to the perpendicular bond is opposite to that due to the parallel bond. The factor of 3 shown that there are three perpendicular bonds in the unit tetrahedron. The number of moving atoms under [111]-directional stress is three (Fig. 1); the effective charge e_b^* due to the bond bending for each moved atom, which corresponds to the second term in Eq. (4), is

$$e_b^* = \tfrac{1}{3}[0.75\Delta\lambda_b^{\parallel} - 3(0.25 - \delta)\,\Delta\lambda_b^{\perp}]/\delta , \tag{12}$$

in units of the elementary charge e_0. For GaAs, e_b^* is 0.32 and for ZnSe it is 0.27. The *plus* sign of e_b^* is demonstrated as follows: For the [111]-directional distortion δ in Fig. 4, we chose that three cations move to the *negative* [111] direction. The negative [111]-directional-cation movement stimulates the increase of $\lambda_b^{\parallel}$. The electron cloud (negative charge) moves to the *positive* [111] direction with the same δ. Thus, the dipole moment induced with $\Delta\lambda_b^{\parallel}$ has the same sign as the dipole moment of the cation (plus charge) motion.

The normalized (dimensionless) piezoelectric charge a^2e_{14}, where a is the cube size,[1] may be given as

$$a^2e_{14} = Z^* + \zeta e_b^* + (\zeta - 1)e_T^* , \tag{13}$$

where $Z^* = 4\lambda - \Delta Z$ is the rigid-ion charge without electron-cloud distortion. ΔZ is the valence-number difference (1 for GaAs and 2 for ZnSe). The last term in Eq. (13) represents the bond-stretching effect. It appears with the motion of the *anion* in Fig. 1 with relation to the cation sublattice. $\zeta = 1$ denotes that the anion in Fig. 1 is perfectly stable, so that the bond stretching effect does not appear. For $\zeta = 0$, the effect due to the anion movement contributes to e_{14} fully with sign opposite to that of Z^*. All values in Eq. (13) are listed in Table V. λ and e_b^* are calculated in this paper. ζ and e_T^* are the experimental values. The correlation between theoretical and experimental values is given in Fig. 5.

IV. DISCUSSION AND SUMMARY

The coincidence between theory and experiment for e_{14} is not so perfect. There are several reasons for this situation. First, the estimation of λ is not so obvious. Our electron localizability λ, based on the Chadi-Cohen parameters, is nearly in agreement with Phillip's ionicity,[9] whereas Pauling's ionicity,[10] which is strongly related to the dipole moment of two-atom molecules, is not correlated to our λ. Second, the values ζ and e_T^* are not so clearly established yet. The last term is the largest of all terms in Eq. (13). Small errors in ζ or e_T^* cause a large error in e_{14}. A more accurate estimate of ζ and e_T^* is welcome.

We use the experimental e_T^* in this paper; there-

TABLE V. Parameters for the calculation of the dimentionless piezoelectric constant a^2e_{14}. λ is the electron localizability, ΔZ is the valence-number difference, Z^* is the rigid-ion charge, ζ is Kleinman's internal displacement parameter, e_T^* is the transverse optical charge, and the last column gives the experimental a^2e_{14} values (Ref. 1).

Crystal	λ	ΔZ	Z^*	ζ [a]	e_b^*	e_T^*	$(\zeta-1)e_T^*$	$Z^*+e_b^*+(\zeta-1)e_T^*$	a^2e_{14} [b]
GaAs	0.357	1	0.428	0.60	0.32	2.16	−0.864	−0.116	−0.32
ZnSe	0.644	2	0.576	0.72	0.27	2.03	−0.562	+0.284	+0.10

[a] Richard M. Martin, Phys. Rev. B 1, 4005 (1970). [b] Reference 1.

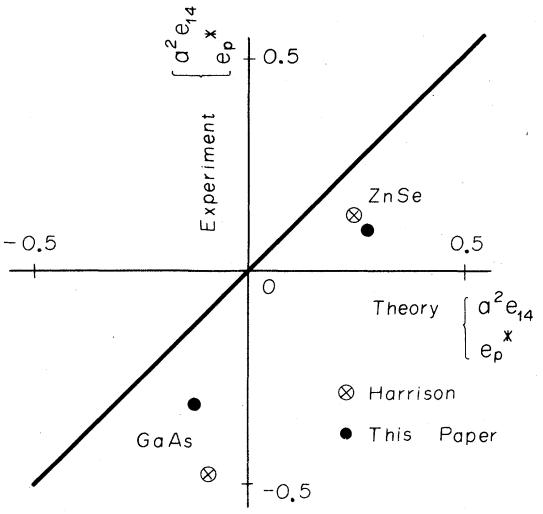

FIG. 5. Experimental piezoelectric charge a^2e_{14} (Ref. 1) and calculated values for GaAs and ZnSe. ● shows ours and ⊗ shows Harrison's a_p^* (Ref. 4).

fore the treatment of the piezoelectric constant in this paper is *semiempirical*. Theoretical calculation of e_T^* by the ELCAO method will be submitted in the future.

The Chadi-Cohen model used in this paper is insufficient because of the lack of all second-nearest-neighbor interactions in the LCAO secular equation. Second-nearest-neighbor interaction means the interaction between the βI and βII cations in Fig. 1(b).[8] The physical importance of the second-nearest-neighbor interaction is as follows: The magnitude of the second-nearest-neighbor interaction is about one order of magnitude smaller than the nearest-neighbor interaction. However, the number of second-nearest-neighbor interactions in the unit cell is three times larger than the number of nearest-neighbor interactions. In Fig. 1 we see that an anion is enclosed by four nearest-neighbor cations, and that one cation is enclosed by 12 cations at the second-nearest-neighbor positions. Second, the change of the second-nearest-neighbor interaction with strain δ may be one order of magnitude larger than the change in the nearest-neighbor interaction.[11] Altogether, the effect of the second-nearest-neighbor interaction may be of the same order as that of the nearest-neighbor interaction.

It is desirable to obtain other lattice-dynamical values such as the shear moduli[6] using the ELCAO method. However, in GaAs and ZnSe, the ionic energy affects more or less the elastic shear moduli, in contrast to the case of C, Si, and Ge.[6] To obtain the shear moduli of partly ionic crystals, we have to calculate them accurately, which is not the aim of this paper.

In summary, the main results of this paper are as follows. First, we calculated the valence-band energy and the electron localizability, using the LCAO method, at the representative points Γ, X, and L. λ_p of the p-like (upper valence) band is different from λ_s of the s-like (lower valence) band. Second, we conclude that the change of λ_p (for the p-like band) is larger than that of λ_s (for the s-like band). This was first pointed out in this paper. Third, the difference of the bond localizability of the parallel bond (to external stress) from that of the perpendicular bond is due to the difference of the s-p hybrid ratio in the respective bonds. The sp^3 hybridization is destroyed under external stress. The bond bending charge e_b^* is of the same order as the piezoelectric constant e_{14} itself.

A recent theoretical treatment[12] of the second-order nonlinear optical susceptibilities $x_{ijk}^{(2)}$ of distorted wurtzite-type crystals such as BeO shows that the electron localizability of the z bond (parallel to the c axis of the wurtzite structure) is different from that of the x bond (perpendicular to the c axis). $\Delta f_i = f_{ix} - f_{iz}$, which may correspond to $\lambda_b^{\perp} - \lambda_b^{\parallel}$ in this paper, is proportional to the spontaneous distortion $\Delta(c/a)$. $\Delta f_i/\Delta(c/a)$ has the same sign and magnitude as $(\lambda_b^{\perp} - \lambda_b^{\parallel})/\delta$ in this paper.

APPENDIX

The s-p hybrid ratio for a distorted tetrahedron is calculated. For simplicity, in Fig. 1(a) we redefine the axis [111] as the Z axis and the axis at 90° perpendicular to the [111] axis as the X axis (in this Appendix only). Then, the bond wave functions ϕ_z and ϕ_x are

$$|\phi_z\rangle = \frac{1}{(1+\mu^2)^{1/2}}\left(|p_z\rangle + \mu|s\rangle\right),$$
$$|\phi_x\rangle = \sqrt{\tfrac{2}{3}}\,|p_x\rangle + \sqrt{\tfrac{1}{3}}\,\frac{1}{(1+\mu^2)^{1/2}}\left(|s\rangle - \mu|p_z\rangle\right), \tag{A1}$$

where μ is the sp^3 hybrid ratio. Since $|p_x\rangle$ has a $\sin\theta$ dependence and $|p_z\rangle$ has a $\cos\theta$ dependence in Fig. 1(a), the θ-dependent part of ϕ_x, $\phi_x(\theta)$, is

$$\phi_x(\theta) = \sqrt{\tfrac{2}{3}}\,\sin\theta + \sqrt{\tfrac{1}{3}}\,\frac{1}{(1+\mu^2)^{1/2}}\,(-\mu\cos\theta). \tag{A2}$$

$\phi_x(\theta)$ has a maximum amplitude in the bond-angle direction; $\partial\phi_x(\theta)/\partial\theta = 0$ leads to $\sqrt{\frac{2}{3}}\cos\theta_b + (1/\sqrt{3})[1/(1+\mu^2)^{1/2}]\sin\theta_b = 0$. After some calculations,

$$\mu^2 = 2/(\tan^2\theta_b - 2) \tag{A3}$$

is obtained. When $\theta_b = 109.5°$ (nondistorted value) is inserted, $\mu = 1/\sqrt{3}$ is obtained (sp^3 hybridiza-

tion). When $\theta_b = 90°$ is assumed, one deduces $\mu = 0$ (sp^2 hybridization).

The weight of the p-type wave function in ϕ_z is $1/(1+\mu^2)$ and that of the s-type one is $\mu^2/(1+\mu^2)$. Therefore, the localizability of the state ϕ_z may be defined as

$$\lambda_b^{\parallel} = \frac{\mu^2}{1+\mu^2}\lambda_s| + \frac{1}{1+\mu^2}\lambda_p| \ , \tag{A4}$$

and also

$$\lambda_b^{\perp} = \frac{1}{3}\frac{1}{1+\mu^2}\lambda_s| + \left(\frac{2}{3} + \frac{1}{3}\frac{\mu^2}{1+\mu^2}\right)\lambda_p| \tag{A5}$$

is obtained for ϕ_x.

$\Delta\theta = \theta_0 - \theta_b = \sqrt{2}\,\delta$ is easily deduced using simple geometrical considerations in Fig. 1. $\delta = 0.05$ (our sample calculation) leads to $\Delta\theta = 4.05°$, and $\mu^2 = 0.7195$:

$$\begin{aligned} \lambda_b^{\parallel} &= 0.152\lambda_s| + 0.848\lambda_p| \ , \\ \lambda_b^{\perp} &= 0.283\lambda_s| + 0.717\lambda_p| \ , \end{aligned} \tag{A6}$$

with distortion $\delta = 0.05$.

[1]Richard M. Martin, Phys. Rev. B 5, 1607 (1972).
[2]G. Arlt and P. Quadflieg, Phys. Status Solidi 25, 323 (1968).
[3]J. C. Phillips and J. A. Van Vechten, Phys. Rev. Lett. 23, 1115 (1969).
[4]Walter A. Harrison, Phys. Rev. B 10, 767 (1974).
[5]B. I. Bennett and A. A. Maradudin, Phys. Rev. B 5, 4146 (1972).
[6]M. Lennoo and J. N. Decarpigny, Phys. Rev. B 8, 5704 (1973).
[7]D. J. Chadi and M. L. Cohen, Phys. Status Solidi B 68, 405 (1975).
[8]J. C. Slater and G. F. Koster, Phys. Rev. 94, 1498 (1954).
[9]J. C. Phillips, Rev. Mod. Phys. 42, 317 (1970).
[10]L. Pauling, *The Nature of the Chemical Bonds* (Cornell University, Ithaca, 1960), Chap. III.
[11]T. Hidaka, Physica (Utr.) B 85, 283 (1977).
[12]T. Hidaka, J. Phys. Soc. Jpn. 43, 1884 (1977).